

Intrastromal Suturing Technique Compared With Interrupted Corneal Suturing Technique, Loose Suture and Knot Exposure: A Comparative Rabbit Study

Surgical Innovation
2025, Vol. 32(4) 325–333
© The Author(s) 2025
Article reuse guidelines:
sagepub.com/journals-permissions
DOI: 10.1177/15533506251328456
journals.sagepub.com/home/sri



Kaan Ozkan, MD^{1,2} , Bahri Aydın, MD¹, Ahmet Yucel Ucgul, MD, FRCS, FEBO, FICO³, Kemal Bayrakceken, MD⁴, Mehmet Cuneyt Ozmen, MD, FICO¹ , and Rustu Fikret Akata, MD¹

Abstract

Purpose: This study aimed to assess the effectiveness of an innovative intrastromal suturing technique in an experimental rabbit model, comparing it to standard interrupted suturing, loose suture, and suturing with knot exposure.

Methods: Fourteen adult male New Zealand White rabbits were included in this study. Each rabbit underwent suturing in both eyes, divided into four groups based on suturing techniques. The novel intrastromal suturing technique involved burying the entire suture material within the corneal stroma. Corneal neovascularisation (CoNV) areas were evaluated by image analysis and immune cell densities by in vivo confocal microscopy (IVCM).

Results: The intrastromal suturing group demonstrated significantly smaller CoNV areas at both 1 week and 1 month post-suturing compared to other interventional groups, indicating effective mitigation of CoNV development and progression. Moreover, this group exhibited lower immune cell densities in the superficial stromal layer and endothelial layer, suggesting a reduced inflammatory response. Both the loose suture and the knot exposure groups exhibited significant levels of CoNV and heightened immune cell densities.

Conclusion: This experimental study demonstrated effectiveness of intrastromal suturing technique in limiting CoNV and immune cell infiltration, common contributors to graft rejection and complications. Furthermore, the study revealed that loose sutures and those with exposed knots are likely to cause more severe CoNV and inflammation, compared to the traditional interrupted suturing technique and intrastromal suturing.

Keywords

corneal neovascularization, immune cell density, intrastromal suturing, rabbit study, standard interrupted suturing

Introduction

Keratoplasty is the gold standard surgical procedure that allows the replacement of a diseased cornea with a clear donor cornea in patients with corneal disorders that lead to significant vision loss or threaten eyeball integrity.¹ Conditions affecting only the corneal stroma can be treated with lamellar keratoplasty, while those affecting the corneal endothelium require endothelial keratoplasty. However, penetrating keratoplasty is necessary if the full-thickness cornea is involved.²

In both penetrating and lamellar keratoplasty, the donor corneal button is usually sutured to the recipient bed using an interrupted or continuous suturing technique.³ Both techniques can give rise to a number of suture-related problems in both the early and late postoperative periods.

Corneal sutures may become loose during the post-operative follow-up secondary to wound healing, corneal dehydration, the cheese-wiring effect, or biodegradation

¹Department of Ophthalmology, School of Medicine, Gazi University, Ankara, Turkey

²Department of Ophthalmology, Training and Research Hospital, Kastamonu University, Kastamonu, Turkey

³Department of Ophthalmology, Training and Research Hospital, Ahi Evran University, Kırşehir, Turkey

⁴Department of Ophthalmology, School of Medicine, Erzincan Binali Yildirim University, Erzincan, Turkey

Corresponding Author:

Kaan Ozkan, MD, Ophthalmology, Kastamonu University, Emniyet Mah, Bandırma Cad. No: 6/1, Yenimahalle/Ankara 06560, Turkey.
Email: ozkakaan91@gmail.com

of 10-0 nylon sutures, even if the proper suturing technique is implemented.⁴ Loose sutures are considered more problematic than tight ones, as they can cause suture-related infectious keratitis, corneal neovascularization (CoNV), immune infiltrates, and resultant graft rejection, all of which largely result from suture erosion through the ocular surface.^{5,6} The resultant graft rejection not only leads to graft dysfunction but also increases the risk of graft rejection after repeated keratoplasty.⁷ Therefore, loose and broken sutures should be removed once they are observed; however, timely management may not always be possible, particularly if regular clinical attendance is less likely. Furthermore, suture removal can be complicated by wound dehiscence and unexpected astigmatism.^{8,9}

Given these complications, cornea specialists are still in search of new solutions to avoid suture-related complications. This novel intrastromal suturing technique enables the suture material to be completely placed inside the corneal stroma, thereby aiming to eliminate the aforementioned suture erosion-related complications.

Therefore, we aimed to evaluate the effect of intrastromal suturing technique in an experimental rabbit study by comparing it with standard interrupted suturing technique, loose suturing and knot exposure. Our assessment includes the measurements of newly-developed corneal neovascularization area after suturing, and immune cells densities in different corneal layers on in vivo confocal microscopy (IVCM).

Materials and Methods

This experimental study followed the guidelines on the care and use of animals adopted by the Society for Neuroscience and Association for Research in Vision and Ophthalmology. The Animal Experiments Local Ethics Committee at the Gazi University (Ankara, Turkey) approved the study (Approval No/Date: 21.047/22.06.2021).

Animals

Fourteen adult male New Zealand White rabbits weighing 3000 to 4000 g were involved in this study. We verified that all rabbits had healthy avascular corneas before the experiment. All rabbits were housed in a room with a 12:12 hour light–dark cycle. Intramuscular ketamine hydrochloride (50 mg/kg) and xylazine (5 mg/kg) were used for deep anaesthesia. Proparacaine hydrochloride 0.5% (Alcaine; Alcon, Fort Worth, TX) was used for topical corneal anaesthesia. Euthanasia was performed using cardiac puncture under deep anaesthesia at the end of the study.

Control and Treatment Groups

Both eyes of each rabbit were included in the study, with different suturing techniques applied to the right and left eyes. This approach was chosen to maximize data collection while minimizing the number of animals used, in accordance with ethical guidelines. We divided the eyes into four groups according to the type of suturing. The right eyes of first 7 rabbits underwent standard interrupted suturing and served as the control group ($n = 7$), whereas the left eyes of them did interrupted suturing with knot exposure ($n = 7$). The right eyes of the remaining rabbits underwent loose suturing ($n = 7$), while the remaining left eyes did intrastromal suturing ($n = 7$). All sutures were placed by a single ophthalmic surgeon (K.Ö.).

Treatment Protocols

Under the operating microscope, a 2-mm length full-thickness incision was made 2 mm anterior to the superior surgical limbus using a straight knife angled at 15° (Storz ophthalmic instruments, Germany). In all groups, each 10-0 nylon suture (Ethicon, Johnson & Johnson, USA) was positioned at a length of 2 mm, with 1 mm on each side of the incision. Three sutures were placed, each 1 mm apart, in each eye. In the control group, sutures traversed the stroma at approximately 90% depth on each side of the incision, and they were tied using an initial triple loop followed by two additional single loops. The knots were buried on the limbal side. In the knot exposure group, suturing was conducted similarly to the control group, but the knot and suture tips remained unburied. In the loose suturing group, a normal tension suture was first positioned in the middle of the incision to prevent leakage. Subsequently, 2.0 prolene suture material (Prolene Blue Monofilament, Ethicon, Johnson & Johnson, USA) was placed on the incision area parallel to the incision line. Two additional sutures, 1 mm away from each side of the initial suture, were tied, covering the prolene suture. The prolene suture was then removed, and confirmation was made that the additional two sutures had come loose. In the intrastromal suturing group, the suture was placed so that the entire suture material was buried inside the stroma. [Figure 1](#) illustrates the detailed steps of the intrastromal suturing technique. At the end of the suturing procedure, the incisions were checked for leakage, and moxifloxacin 0.5% (Vigamox, Alcon Laboratories) was instilled four times a day for 1 month for bacterial prophylaxis.

Analysis of CoNV Area

On the first week and first month, standard images were captured at 10× magnification using software (Avermedia, Taiwan) attached to the operating microscope

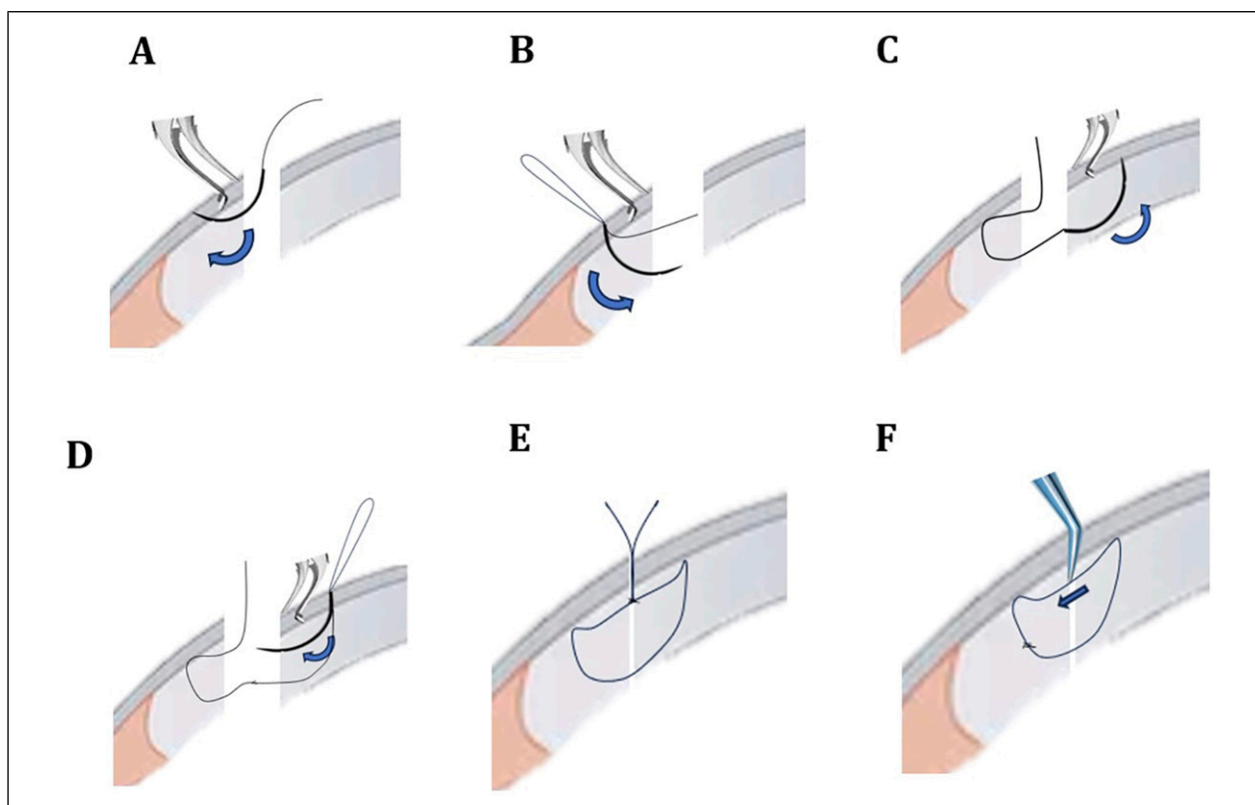


Figure 1. The basic steps of the intrastromal suturing technique. (A) A 10.0 nylon suture passes through 20-30% of the recipient bed's depth. (B) The needle re-enters the ocular surface at the same point where it previously exited, passing through 90% of the recipient. (C) A 10.0 nylon suture passes through 90% of the donor button's depth. (D) The needle re-enters the donor surface at the same point where it previously exited, passing through 20-30% of the donor button's depth. (E) The suture is tied with a triple loop followed by two additional single loops. (F) The suture is buried on the limbal side.

(Möller-Wedel FS 3000, Haag Streit, Switzerland). To standardize the area calculation, a millimetre ruler was positioned in the vicinity of the CoNV area. Two masked researchers (K.Ö and A.Y.U.) manually delineated the CoNV area and measured its size using the Image J program (Figure 2).¹⁰ The average of the two measurements was considered for statistical analysis.

Analysis of IVCN Images

The Rostock Cornea Module, attached to the Heidelberg Retina Tomograph III (HRT III RCM) (Heidelberg Engineering GmbH, Dossenheim, Germany), was utilized for IVCN. Following the application of carbomer gel (Viscotears; Fribourg, Switzerland) to the front surface of the microscope lens and ensuring the absence of air bubbles, a single-use TomoCap® was mounted, and a second drop of ophthalmic gel was placed on the outer surface of the TomoCap®. Images were acquired from the superficial stromal layer (corresponding to the region where the Bowman's layer is located in species that have this structure) and the endothelial layer of the cornea with a field size of $400 \times 400 \mu\text{m}$, which primarily captured the central and paracentral cornea. Due to technical

limitations, direct imaging of the peripheral cornea where sutures were placed was not feasible. Immune cells were defined as round, dense, hyper-reflective cells with a size of 10 microns and larger, referencing a previous study.¹¹ Immune cell densities were measured using the ImageJ program. Initially, immune cells were automatically selected using the thresholding method. Subsequently, the image was binarized to display only immune cells, and immune cells were counted automatically using ROI Manager in the Image J program. Finally, the number of immune cells per mm^2 (immune cell density) was calculated (Figure 3). To ensure consistency in immune cell density measurements, all IVCN images were captured as perpendicular to the corneal surface as possible. Minor variations in imaging angle were unavoidable due to corneal curvature. To correct for these variations, immune cell density calculations were standardized by expressing cell counts per mm^2 , normalizing for differences in image capture area. Additionally, excessively oblique or distorted images were excluded from analysis.

Furthermore, a comprehensive ophthalmic examination was performed on all rabbits at each follow-up visit. This included slit-lamp biomicroscopy to assess for signs of anterior uveitis, such as aqueous flare or keratic precipitates.

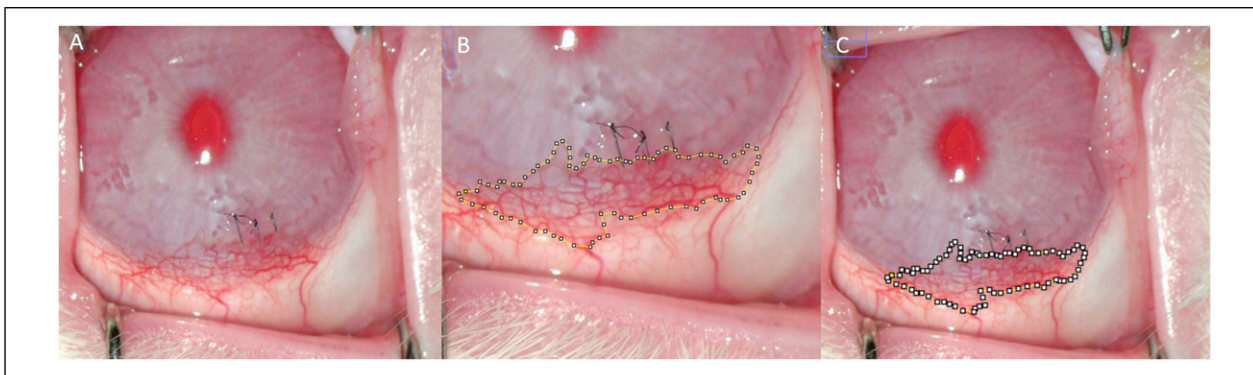


Figure 2. Method for calculating the area of corneal neovascularization. (A) A standard magnification image of the CoNV area, unmarked. (B) A magnified view of the CoNV area, delineated with manual markings. (C) A standard magnification image of the CoNV area with markings.

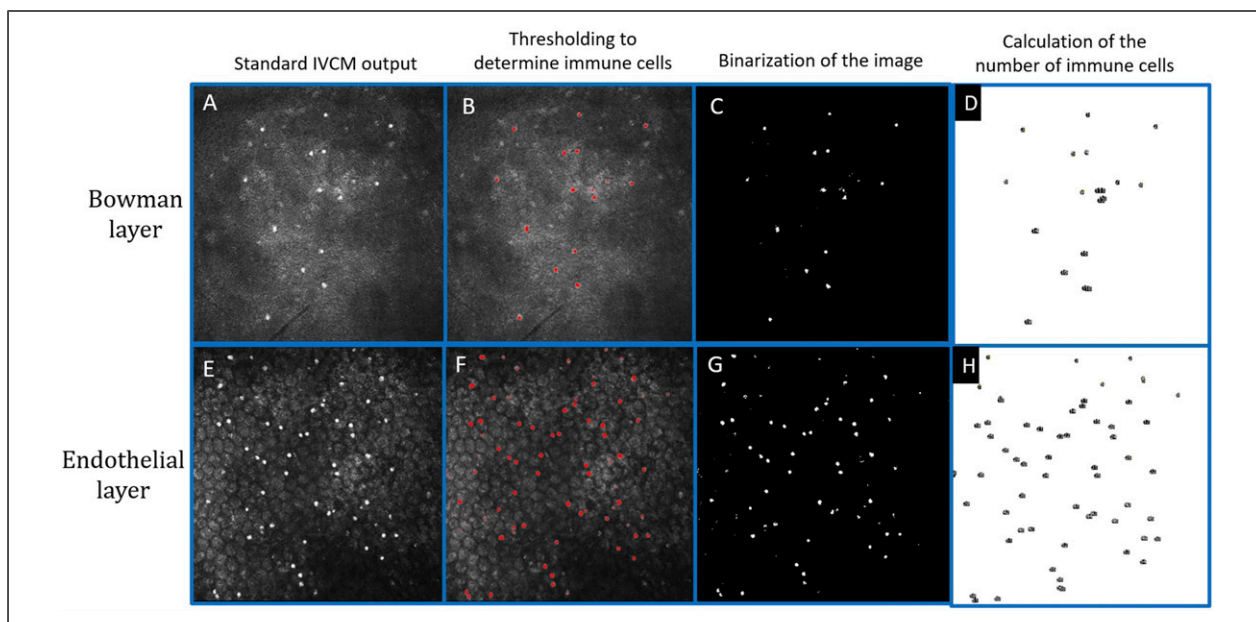


Figure 3. Method for calculating immune cell density. (A) A standard IVCM image of the superficial stromal layer. (B) Thresholding separates the immune cells from other structures in the superficial stromal layer. (C) The image is binarized, making only the immune cells visible. (D) Immune cell count in the superficial stromal layer is calculated. (E) A standard IVCM image of the endothelial layer. (F) Thresholding separates the immune cells from other structures in the endothelial layer. (G) The image is binarized, making only the immune cells visible. (H) Immune cell count in the endothelial layer is calculated.

Statistical Analysis

Before commencing the experiment, the sample size of each group was determined, considering the power of each analysis to be ≥ 0.8 using Gpower 1.3.9.4 version software. The collected data from the present study were analysed using SPSS software for Windows version 22.0 (Chicago, IL). The Kruskal-Wallis test was employed to compare the CoNV areas and immune cell densities among the groups. Additionally, Tamhane's T2 post hoc test was utilized for pairwise comparisons. Outcomes were presented using boxplots due to the nonparametric

distribution of the collected data. A *P*-value less than 0.05 was considered statistically significant.

Results

Morphologic Evaluation of CoNV Area

The development of corneal neovascularization (CoNV) varied in intensity among all eyes subjected to suturing. However, the CoNV area was notably smaller in the intrastromal suturing group during the first week, measuring $3.8 \pm 2.0 \text{ mm}^2$. This was significantly less compared to the

other groups, where the CoNV areas were $11.8 \pm 3.9 \text{ mm}^2$ in the control group, $17.8 \pm 4.9 \text{ mm}^2$ in the knot exposure group, and $16.8 \pm 5.9 \text{ mm}^2$ in the loose suturing group ($P = 0.022$, Figure 4A). Moving to the first month, the CoNV area slightly increased to $4.2 \pm 1.6 \text{ mm}^2$ in the intrastromal suturing group but remained markedly smaller than the other groups. Specifically, the CoNV areas were $13.5 \pm 3.6 \text{ mm}^2$ in the control group, $16.7 \pm .3 \text{ mm}^2$ in the knot exposure group, and $18.7 \pm 3.8 \text{ mm}^2$ in the loose suturing group ($P = 0.037$, Figure 4C). Figure 5 displays representative anterior segment images for all groups at both the first week and the first month.

Evaluation of Immune Cell Density

Immune cells infiltrated the corneal layers in all eyes 1 month after suturing. Examining immune cell density in the superficial stromal layer, it was $33.2 \pm 13.8 \text{ cells/mm}^2$ in the intrastromal suturing group, which was lower compared to the other groups ($46.4 \pm 12.3 \text{ cells/mm}^2$ in the control group, $78.8 \pm 22.7 \text{ cells/mm}^2$ in the knot exposure group, and $75.7 \pm 24.1 \text{ cells/mm}^2$ in the loose

suturing group, $P = 0.004$, Figure 4B). The immune cell density in the endothelial layer was $32.7 \pm 13.5 \text{ cells/mm}^2$, similar to that of the superficial stromal layer in the intrastromal group; however, it was still lower than those in endothelial layers in the other groups ($46.7 \pm 14.8 \text{ cells/mm}^2$ in the control group, $44.2 \pm 19.0 \text{ cells/mm}^2$ in the knot exposure group, and $46.1 \pm 16.5 \text{ cells/mm}^2$ in the loose suturing group, $P = 0.008$, Figure 4D). Figure 6 displays representative IVCM images in all groups at both the superficial stromal layer and the endothelial layer.

No clinical signs of anterior uveitis, such as aqueous flare or keratic precipitates were observed in any rabbits during the follow-up period.

Discussion

The present study introduces a novel intrastromal suturing technique designed to mitigate suture-related complications. The evaluation of this technique in an experimental rabbit model provides valuable insights into its potential benefits compared to standard interrupted suturing. The morphologic evaluation revealed a significant reduction

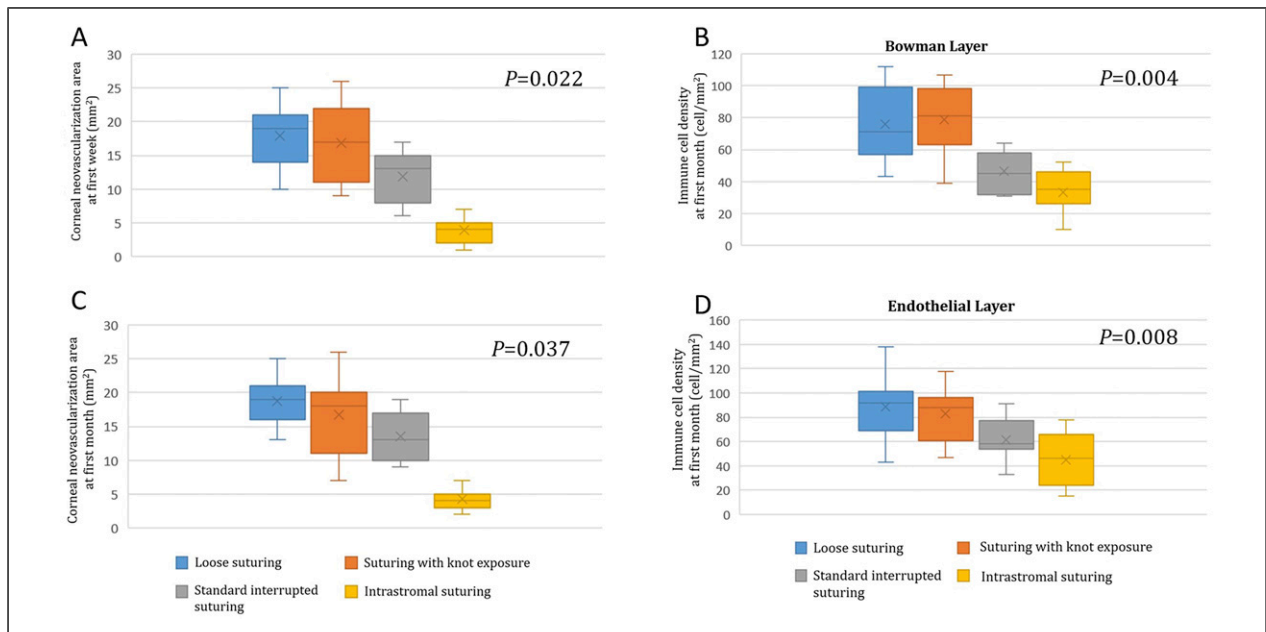


Figure 4. Corneal neovascularization areas and immune cell densities in the groups. (A) CoNV areas at the first week in each group. In pairwise comparison of each group with the intrastromal suturing group, $P < 0.001$ for the intrastromal suturing group vs the control group, $P < 0.001$ for the intrastromal suturing group vs the knot exposure group, and $P < 0.001$ for the intrastromal suturing group vs the loose suturing group. (B) Immune cell densities at the first month in the superficial stromal layer in each group. In pairwise comparison of each group with the intrastromal suturing group, $P = 0.036$ for the intrastromal suturing group vs the control group, $P < 0.001$ for the intrastromal suturing group vs the knot exposure group, and $P < 0.001$ for the intrastromal suturing group vs the loose suturing group. (C) CoNV areas at the first month in each group. In pairwise comparison of each group with the intrastromal suturing group, $P < 0.001$ for the intrastromal suturing group vs the control group, $P < 0.001$ for the intrastromal suturing group vs the knot exposure group, and $P < 0.001$ for the intrastromal suturing group vs the loose suturing group. (D) Immune cell densities at the first month in the endothelial layer in each group. In pairwise comparison of each group with the intrastromal suturing group, $P = 0.047$ for the intrastromal suturing group vs the control group, $P = 0.004$ for the intrastromal suturing group vs the knot exposure group, and $P = 0.003$ for the intrastromal suturing group vs the loose suturing group.

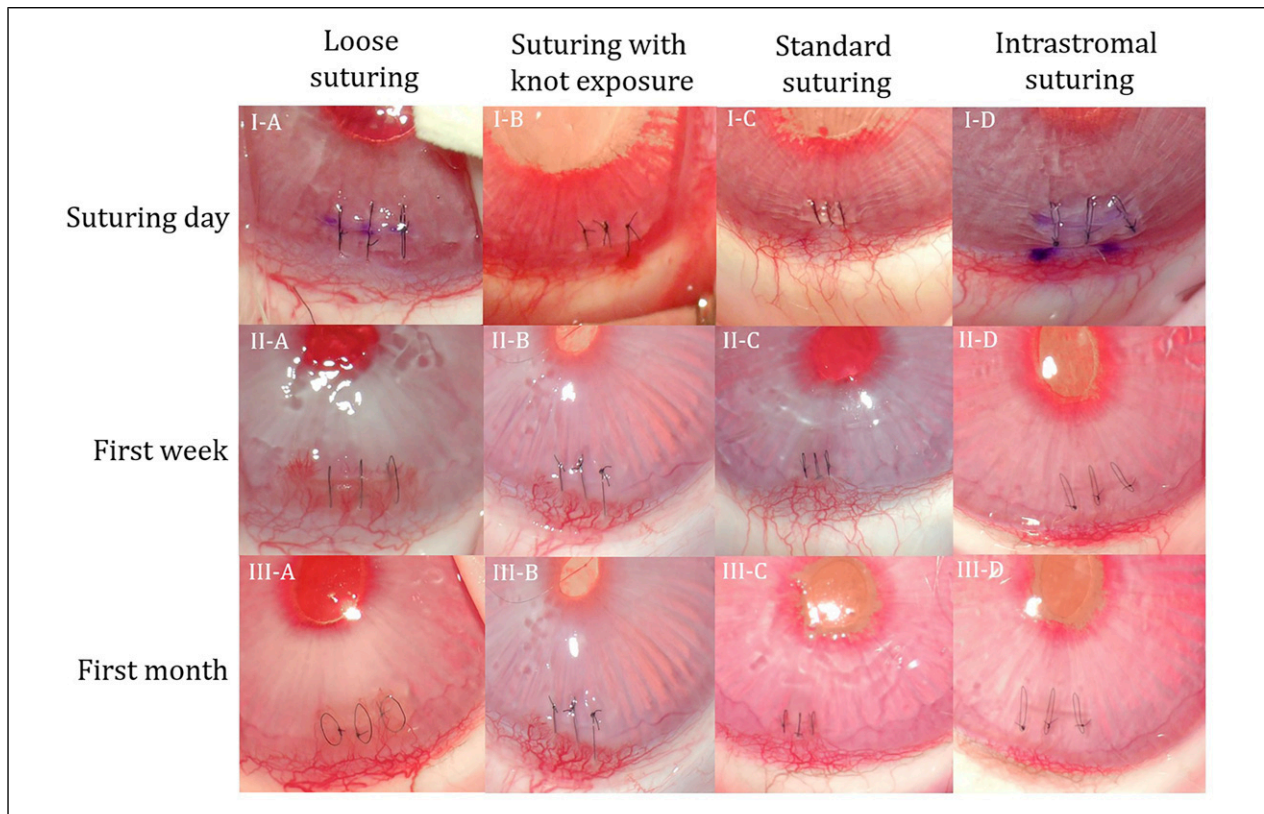


Figure 5. Representative images of each group at different time point. IA- Appearance of sutures shortly after the completion of loose suturing. IB- Visualization of sutures soon after completing the suturing process, characterized by exposed knots. IC- Appearance of sutures shortly after the completion of standard interrupted suturing. ID- This image shows the sutures as visualized soon after completing the intrastromal suturing technique. IIA- Neovascular vessels sprouting into loose sutures at the first week. IIB- Exposed knots leading to the development of CoNV at the first week. IIC- CoNV reaching the suturing area 1 week after standard interrupted suturing. IID- Minimal CoNV development not reaching the suturing area 1 week after intrastromal suturing. IIIA- Neovascular vessels sprouting beyond loose sutures at the first month. IIIB- CoNV area increased in density in the first month compared to the first week. IIIC- CoNV remained unchanged from the first week to the first month. IIID- CoNV area decreased in size and density from the first week to the first month.

of the CoNV area in the intrastromal suturing group compared to other groups at both 1 week and 1 month post-suturing. This outcome suggests that the novel technique effectively limits the development and progression of CoNV. The smaller area of CoNV observed in the intrastromal suturing group is particularly promising, as excessive corneal neovascularization can compromise corneal transparency and lead to the rejection of corneal transplant grafts. Furthermore, this study has also shown that CoNV is significantly present in both loose suturing and knot exposure cases. These results indicate that loose suturing stimulates corneal neovascularization as markedly as knot exposure does, thereby explaining why it is considered an alarming sign.

The infiltration of immune cells in the corneal layers is a crucial aspect of the inflammatory response. The intrastromal suturing group demonstrated lower immune cell densities in both the superficial stromal and endothelial layers compared to other groups. This finding

suggests that the novel suturing technique may elicit a reduced inflammatory response, potentially minimizing the risk of complications associated with immune cell infiltration, such as graft rejection. In clinical settings, this may be particularly beneficial in paediatric keratoplasties where postoperative inflammation and immune reaction can be extensive. Moreover, similarly to the induction of CoNV, it appears that loose suturing plays a significant role in stimulating the immune response as knot exposure does.

A well-tied nylon suture, known to be resistant to hydrolysis and biological degradation over time, extends smoothly on the corneal surface to eventually become covered by epithelial cells, with its knot embedded in the stroma. It is known that the superficial portion of a nylon suture left in the cornea tends to undergo earlier hydrolysis and biological degradation compared to its deeper portion.¹² Superficial sutures left in the cornea can lead to subepithelial fibrosis and an inflammatory reaction due to

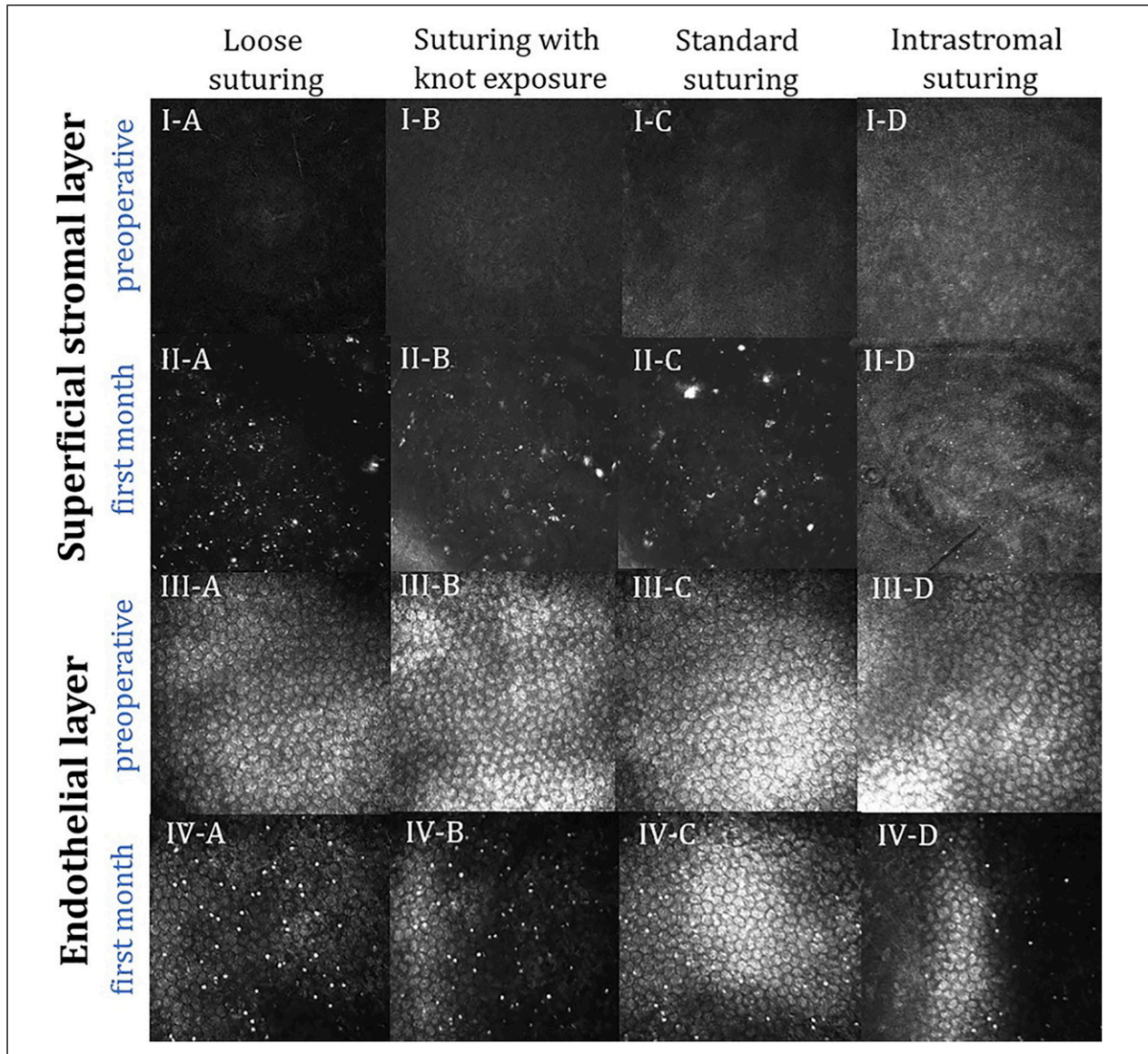


Figure 6. Representative IVCM images of each group. IA, IB, IC, and ID illustrate the superficial stromal layers of the rabbits in each group prior to the experiment. Similarly, IIIA, IIIB, IIIC, and IIID depict the endothelial layers. Notably, both layers lack immune cells. IIA and IVA reveal significant immune cell infiltration in the superficial stromal and endothelial layers, respectively, for the loose suturing group. IIB and IVB display similar infiltration in the knot exposure group. In the standard suturing group, IIC and IVC demonstrate moderate immune cell infiltration in the superficial stromal and endothelial layers, respectively. IID and IVD indicate relatively lower immune cell infiltration in the superficial stromal and endothelial layers, respectively, for the intrastromal suturing group, compared to the other groups.

late suture loosening.¹³ Following penetrating keratoplasty performed using the standard interrupted suture technique, sutures tend to loosen for various reasons, resulting in suture erosion on the ocular surface. In the early stages, inadequate tightening during suturing and changes in corneal hydration balance are among the main causes of suture loosening. In the later stages, sutures may loosen due to incomplete epithelial barrier formation along the suture line, allowing microorganisms to penetrate the stroma and cause infiltrates. Moreover, late suture

loosening and breakage can occur due to biodegradation of the nylon suture material. Ultimately, superficial sutures may contribute to epithelial erosion.¹³

Christo et al⁴ reported suture loosening at a rate of 8.3%, suture erosion at 10.8%, suture-related sterile infiltrates at 9.4%, and suture-related infectious keratitis at 3.3% in 361 cases of penetrating keratoplasty with an average follow-up of 4.2 years in 332 patients. Furthermore, Crawford et al¹⁴ observed suture erosion, loosening, or breakage in 31% of patients with an average

follow-up of 40 months after 913 keratoplasties. Singar et al¹⁵ noted that 59 out of 633 patients who underwent penetrating keratoplasty required resuturing, with loose sutures being the most common reason, accounting for 63% of cases. Moreover, Sharma et al¹⁶ emphasized that suture loosening is a significant risk factor for graft rejection and highlighted the role of corneal neovascularization and suture infiltrates in the rejection mechanism. The underlying pathological mechanism is attributed to the suture material itself being angiogenic or mechanical stress-induced angiogenic substance secretion in epithelial cells due to interaction between the unepithelialized suture material and surrounding tissue, as well as the attraction of lymphocytes and macrophages by sutures, leading to the secretion of angiogenic substances following complications and intense inflammation.^{17,18} Similarly, the knot exposure and loose suturing groups in this study showed significant CoNV and immune cell infiltration. Furthermore, Bachmann et al¹⁹ conducted a meta-analysis of 24 944 keratoplasties across 19 studies and found that the presence of corneal neovascularization increased the risk of graft failure by 1.32 times and graft rejection by 2.07 times. They also noted that as the number of quadrants involved increased, the risk of rejection also increased.

In paediatric keratoplasty, almost all cases show early suture loosening post-surgery. Therefore, it is recommended to remove the sutures within the first 3 months.²⁰ Following paediatric keratoplasty, there is a 10-50% occurrence of microbial keratitis and a 12-43.4% rate of graft rejection, most of which develop secondarily to loose sutures.²¹ In light of this knowledge, the use of intrastromal suturing techniques, which prevent suture erosion, CoNV development, and excessive immune response, becomes even more valuable in cases of paediatric keratoplasty.

To prevent suture-related complications, Busin et al²² initially performed suturing using an intrastromal suture technique on 17 patients with keratoconus. In this technique, the suture entered the midstroma and exited from the endothelium, then reentered the midstroma from the opposite side and was tied. Not all of the suture was placed within the intrastromal region, as a portion was left in the anterior chamber. Sutures were removed at 3 months, and the patients' refractive outcomes were evaluated. The average endothelial cell loss was 22.4%, and no suture complications were observed in any of the patients. However, in our intrastromal suturing technique, the entire suture remains within the intrastromal area, ensuring no damage to the endothelium.

This study has certain limitations that should be acknowledged. The experimental nature of the model in rabbits may not fully represent the complexities and variations encountered in human keratoplasty.

Additionally, the short-term follow-up in this study may not capture potential long-term complications or benefits associated with the intrastromal suturing technique. Moreover, the intrastromal suture technique is technically more challenging compared to the traditional suture techniques commonly used in penetrating keratoplasties. Furthermore, removing sutures can be challenging since the entire suture is buried intrastromally. Astigmatic management can be achieved using YAG laser suturolysis or with a needle cut without the need for suture removal. As we know from other suture techniques, suture remnants left in the intrastromal area degrade very slowly and rarely lead to complications. Another unknown aspect of this technique is the long-term stabilization of sutures and their astigmatic effects. While this study focused on evaluating the immune response and neovascularization induced by different suturing techniques, we acknowledge that keratoplasty involves additional immune challenges, such as immune reaction to donor tissue, which is critical in the success or failure of corneal transplantation. Future research incorporating rabbit corneal transplant models is recommended to explore the combined effects of donor tissue and suturing techniques on immune activation, neovascularization, and graft survival.

Furthermore, we acknowledge that corneal topography and astigmatism are important considerations in keratoplasty, particularly in pediatric cases where corneal shape significantly influences postoperative visual outcomes. In our study, we did not assess corneal topographic changes, and therefore, we cannot determine whether the intrastromal suturing technique induces higher astigmatism compared to other techniques. Future studies should incorporate corneal topography and astigmatic assessments to better understand the biomechanical effects of different suturing techniques and their long-term implications for corneal stability and visual outcomes.

In conclusion, the intrastromal suturing technique demonstrates promising results in reducing CoNV and immune cell infiltration in an experimental rabbit model. In clinical translation, these findings suggest potential benefits in minimizing suture-related complications associated with traditional keratoplasty techniques. Further clinical investigations are necessary to validate these outcomes and assess the long-term safety and efficacy of the intrastromal suturing technique in human subjects.

Author Contributions

KO, BA, MCO, and RFA designed and conducted the study. KO and AYU made significant contribution to image analysis and statistical analysis. KO, AYU and KB wrote the manuscript. All authors read and approved the final manuscript.

Declaration of Conflicting Interests

The author(s) declared no potential conflicts of interest with respect to the research, authorship, and/or publication of this article.

Funding

The author(s) received no financial support for the research, authorship, and/or publication of this article.

Ethical Statement

Ethical Approval

The Animal Experiments Local Ethics Committee at the Gazi University approved the study.

ORCID iDs

Kaan Ozkan  <https://orcid.org/0000-0002-9617-6961>

Mehmet Cuneyt Ozmen  <https://orcid.org/0000-0002-3164-6336>

References

- Musa M, Zeppieri M, Enaholo ES, Chukwuyem E, Salati C. An overview of corneal transplantation in the past decade. *Clin Pract*. 2023;13(1):264-279. doi:10.3390/clinpract13010024
- Shams M, Sharifi A, Akbari Z, Maghsoudlou A, Reza Tajali M. Penetrating keratoplasty versus deep anterior lamellar keratoplasty for keratoconus: a systematic review and meta-analysis. *J Ophthalmic Vis Res*. 2022;17(1):89-107. doi:10.18502/jovr.v17i1.10174
- Pagano L, Shah H, Al Ibrahim O, et al. Update on suture techniques in corneal transplantation: a systematic review. *J Clin Med*. 2022;11(4):1078. doi:10.3390/jcm11041078
- Christo CG, van Rooij J, Geerards AJ, Remeijer L, Beekhuis WH. Suture-related complications following keratoplasty: a 5-year retrospective study. *Cornea*. 2001;20(8):816-819. doi:10.1097/00003226-200111000-00008
- Dana MR, Goren MB, Gomes JA, Laibson PR, Rapuano CJ, Cohen EJ. Suture erosion after penetrating keratoplasty. *Cornea*. 1995;14(3):243-248. doi:10.1097/00003226-199505000-00003
- Lam VM, Nguyen NX, Martus P, Seitz B, Kruse FE, Cursiefen C. Surgery-related factors influencing corneal neovascularization after low-risk keratoplasty. *Am J Ophthalmol*. 2006;141(2):260-266. doi:10.1016/j.ajo.2005.08.080
- Maguire MG, Stark WJ, Gottsch JD, et al. Risk factors for corneal graft failure and rejection in the collaborative corneal transplantation studies. Collaborative Corneal Transplantation Studies Research Group. *Ophthalmology*. 1994;101(9):1536-1547. doi:10.1016/s0161-6420(94)31138-9
- Renucci AM, Marangon FB, Culbertson WW. Wound dehiscence after penetrating keratoplasty: clinical characteristics of 51 cases treated at Bascom Palmer Eye Institute. *Cornea*. 2006;25(5):524-529. doi:10.1097/01.icc.0000214232.66979.c4
- Chaurasiya SK, Reddy JC, Vaddavalli PK, Rapuano CJ. Changes in post-keratoplasty astigmatism after suture removal: refraction vs tomography vs aberrometry. *Int J Ophthalmol*. 2021;14(11):1707-1713. doi:10.18240/ijo.2021.11.09
- Schneider CA, Rasband WS, Eliceiri KW. NIH image to ImageJ: 25 years of image analysis. *Nat Methods*. 2012;9(7):671-675. doi:10.1038/nmeth.2089
- Chirapapaisan C, Abbouda A, Jamali A, et al. In vivo confocal microscopy demonstrates increased immune cell densities in corneal graft rejection correlating with signs and symptoms. *Am J Ophthalmol*. 2019;203:26-36. doi:10.1016/j.ajo.2019.02.013
- Acheson JF, Lyons CJ. Ocular morbidity due to monofilament nylon corneal sutures. *Eye*. 1991;5(Pt 1):106-112. doi:10.1038/eye.1991.20
- Brightbill FS, McDonnell PJ, McGhee CN, Farjo AA, Serdarevic O. *Corneal Surgery E-Book: Theory Technique and Tissue*. Amsterdam: Elsevier Health Sciences; 2008.
- Crawford AZ, Meyer JJ, Patel DV, Ormonde SE, McGhee C. Complications related to sutures following penetrating and deep anterior lamellar keratoplasty. *Clin Exp Ophthalmol*. 2016;44(2):142-143. doi:10.1111/ceo.12635
- Singar E, Burcu A, Tamer-Kaderli S, Yalınız-Akkaya Z, Ozbek-Uzman S, Ormek F. Resuturing after penetrating keratoplasty without trauma: indications and results. *J Fr Ophthalmol*. 2020;43(1):18-24. doi:10.1016/j.jfo.2019.07.004
- Sharma N, Kandar AK, Singh Titiyal J. Stromal rejection after big bubble deep anterior lamellar keratoplasty: case series and review of literature. *Eye Contact Lens*. 2013;39(2):194-198. doi:10.1097/ICL.0b013e31824ccb91
- Cursiefen C, Chen L, Borges LP, et al. VEGF-A stimulates lymphangiogenesis and hemangiogenesis in inflammatory neovascularization via macrophage recruitment. *J Clin Invest*. 2004;113(7):1040-1050. doi:10.1172/JCI20465
- Cursiefen C, Rummelt C, Kuchle M. Immunohistochemical localization of vascular endothelial growth factor, transforming growth factor alpha, and transforming growth factor beta1 in human corneas with neovascularization. *Cornea*. 2000;19(4):526-533. doi:10.1097/00003226-200007000-00025
- Bachmann B, Taylor RS, Cursiefen C. Corneal neovascularization as a risk factor for graft failure and rejection after keratoplasty: an evidence-based meta-analysis. *Ophthalmology*. 2010;117(7):1300-1305. doi:10.1016/j.opht.2010.01.039
- Trief D, Marquezan MC, Rapuano CJ, Prescott CR. Pediatric corneal transplants. *Curr Opin Ophthalmol*. 2017;28(5):477-484. doi:10.1097/ICU.0000000000000393
- Vanathi M, Raj N, Kusumesh R, Aron N, Gupta N, Tandon R. Update on pediatric corneal diseases and keratoplasty. *Surv Ophthalmol*. 2022;67(6):1647-1684. doi:10.1016/j.survophthal.2022.07.010
- Busin M, Arffa RC. Deep suturing technique for penetrating keratoplasty. *Cornea*. 2002;21(7):680-684. doi:10.1097/00003226-200210000-00009